Food Packaging and Shelf Life 34 (2022) 101003

Contents lists available at ScienceDirect

Food Packaging and Shelf Life

journal homepage: www.elsevier.com/locate/fpsl

Antioxidant poly (lactic acid) films with rice straw extract for food packaging applications

Pedro A.V. Freitas *, Nuria Julia Bas Gil, Consuelo González-Martínez, Amparo Chiralt

Institute of Food Engineering for Development, Universitat Politècnica de València, 46022 Valencia, Spain

ARTICLE INFO

Keywords:
Phenolic compounds
Active food packaging
Bioactive extract
Release kinetics
Ultrasound extraction
Heating method

ABSTRACT

Antioxidant PLA films incorporating 2%, 4% and 6% of phenol-rich extract from rice straw (RS) were obtained by melt blending and compression-moulding. Aqueous RS extract was obtained by a combined ultrasound-reflux heating method and characterised as to its total phenolic content (TPC) and antioxidant capacity. The effect of the extract ratio on the functional properties of the films was analysed, as well as the release kinetics of antioxidants in food simulants (ethanol 10% and 50%). Extract incorporation slightly reduced the strength of the polymer matrix, stretchability, resistance to break, barrier capacity and thermostability, while films became brownish and gained antioxidant capacity. Phenolic compounds from the extract were effectively released into food simulants, depending on the extract concentration, the food simulant and contact time. The radical scavenging capacity of the films reached asymptotic values from about 150 h contact time, and films with 6% of the extract exhibited similar values for both simulants. So, PLA films with approximately 6% of extract could be used as biodegradable active packaging material with antioxidant capacity in both aqueous foods (simulant A) and more fatty products (simulant D1). Further studies are required to verify the antioxidant efficiency of the films in real foods.

1. Introduction

Oxidative reactions, microbial growth, and metabolism are the main factors that lead to a loss of quality and the deterioration of foodstuffs, producing waste (Han et al., 2018). Food spoilage through oxidative processes occurs when food is exposed to air, heat or light, producing reactive oxygen species that damage chemical structures, such as proteins, lipids and vitamins (Marzlan et al., 2022; Lourenço et al., 2019). Oxidative reactions can promote food discoloration and lead to a decrease in nutritional value, as well as produce off-odours and off-flavours (Han et al., 2018; Moreno et al., 2018). To overcome these problems, and despite their potential adverse effects on human health, the food industry often uses synthetic antioxidants due to their stability, availability and low cost (Botterweck et al., 2000; Randhawa & Bahna, 2009). The application of non-synthetic antioxidants for food preservation purposes is a current growing trend since consumers increasingly demand healthier and safer food products incorporating natural substances. Of the natural plant antioxidants, phenolic extracts obtained from agri-food residues or by-products represent an interesting alternative. Obtaining active extracts from these residues contributes to proper environmentally-friendly waste management, produces added-value materials and boosts the circular bioeconomy (Arun et al., 2020). Several studies have been reported to obtain plant extracts from agri-food residues with bioactive properties, such as spinach by-products (Derrien et al., 2017), berry leaves (Ziemlewska et al., 2021), winemaking by-products (Troilo et al., 2021; Jara-Palacios et al., 2020), saffron stigma (Lahmass et al., 2018), rice and coffee husks (Collazo-Bigliardi et al., 2019), and rice straw (Freitas et al., 2020; Menzel et al., 2020).

Of the agro-industrial residues worldwide, the second most widely-produced is rice straw (RS) (*Oryza sativa* L.). The Food and Agriculture Organization of the United Nations (FAO) concluded that global rice production reached approximately 782 million tons, 90% of which was from the Asian continent (FAOSTAT, 2018). Considering that one kilogram of rice grain provides 1.5 kg of RS (Peanparkdee & Iwamoto, 2019), around 1173 million tons of problematic waste, without any monetary value that is difficult to manage, is produced every year. This leads to a continuous increase in air pollution, as the primary destination of this by-product is to be burnt on the paddies, releasing harmful dioxins, such as polychlorinated dibenzo-*p*-dioxins, dibenzofurans, and

* Corresponding author.
E-mail address: pedroafreitas3@gmail.com (P.A.V. Freitas).

https://doi.org/10.1016/j.fpsl.2022.101003
Received 11 April 2022; Received in revised form 2 November 2022; Accepted 21 November 2022
Available online 25 November 2022

greenhouse gas emissions (CH_4, CO_2, and N_2O), thus promoting global warming and affecting human health (Yang et al., 2006). Since RS is a lignocellulosic-rich material (39% cellulose, 20% lignin, 23% hemicellulose, and 15% ashes), alternative waste management can be applied with a focus on waste valorisation and the minimisation of environmental impacts (El-Tayeb et al., 2012).

Obtaining phenolic-rich extracts from RS is a promising alternative for the valorisation of RS since the extracted phenolic compounds have been shown to exhibit high antioxidant capacity and antimicrobial activity (Barana et al., 2016; Karimi et al., 2014). Likewise, it is imperative to optimise the main extraction parameters, such as type of solvent, pre-treatments, temperature, time, and pressure. In fact, the processing factors directly affect the extraction efficiency of phenolic compounds, originally esterified or etherified with the lignocellulosic matrix, especially hemicellulose and lignin. Freitas et al. (2020) reported that the ultrasound pre-treatment of RS water dispersion, followed by water reflux extraction, promoted significant damage to the RS cell tissue, giving rise to an aqueous extract with high phenolic content and antioxidant capacity. These phenolic-rich RS extracts can be used for food formulation or can be incorporated into biodegradable food packaging materials to minimise or delay oxidative processes in foods, as well as to replace synthetic antioxidants.

Biodegradable, economic, and sustainable packaging systems are being proposed to induce more efficient and eco-friendly alternatives to the use of non-biodegradable petroleum-based plastics (Balaji et al., 2018). Poly (lactic acid) (PLA) is a bio-based biodegradable polyester currently ranked in first place in the bioplastics market with a percentage of 18.7% of the total production of bioplastics (European Bioplastics nova-Institute,2020). PLA is included in the group of thermoplastic biopolymers with good barrier and mechanical properties, such as a high resistance to break. Furthermore, PLA has a relatively hydrophobic structure compared with other biopolymers, dissolves fairly easily in solvents such as chloroform, and does not dissolve in water, alcohols, or alkanes (Avérous et al., 2001). PLA has been studied for the purposes of applying it in active food packaging with antioxidant (Jamshidian et al., 2012a,b; Bassani et al., 2019) and antimicrobial properties (Muller et al., 2017a; Vasile et al., 2019; Llana-Ruiz-Cabello et al., 2015). Different processing methods have been used to incorporate bioactive compounds into polymer matrices to provide them with active properties, including solvent casting, electrospinning, supercritical impregnation or spin coating, (Velásquez et al., 2021). However, the incorporation of active compounds into the polymer master batch, by melt blending with thermoplastic polymers, represents a cheaper approach with respect to the other techniques, leading to a good standardization of the active material and being more applicable at industrial scale. The challenge with this method is to maintain bioactivity of the usually thermolabile compounds.

The aim of this study was to obtain PLA-based bioactive films, incorporating phenolic-rich aqueous extract from RS obtained by the combined ultrasound-reflux heating method. PLA films were characterised as to their functional properties; typically, their microstructural, optical, thermal, and barrier properties. Likewise, the release kinetics of phenolic compounds from the PLA active films and their radical scavenging capacity were analysed in two food simulants (aqueous ethanol solutions at 10% and 50%).

2. Material and methods

2.1. Materials

Amorphous PLA 4060D, density 1.24 g/cm^3, an average molecular weight of 106,226 D, with 40% low molecular weight fraction (275 D), was purchased from Natureworks (U.S.A). Ethanol and methanol were supplied by Sigma-Aldrich (Sigma-Aldrich Chemie, Steinheim, Germany). Folin-Ciocalteu reagent, 2,2-Diphenyl-1-pikryl-hydrazyl (DPPH) and Poly (ethylene glycol) (PEG1000) were purchased from Sigma-Aldrich (St. Louis, MO, USA). Sodium carbonate (Na_2CO_3) and magnesium nitrate ($Mg(NO_3)_2$) were obtained from PanReac Química S.L.U (Castellar del Vallés, Barcelona, Spain). di-Phosphorous pentoxide (P_2O_5) was obtained from VWR Chemicals (Belgium).

2.2. Extract preparation

The plant extract was obtained using a previously described method (Freitas et al., 2020). RS (*Oryza sativa L.*), supplied by the straw bank of Valencia (Spain) and obtained from L'Albufera rice fields, was dried at 50 ± 2 ℃, under vacuum (0,8 mmbar) for 20 h. Afterwards, the dried RS was milled using a milling machine (IKA, model M20, Germany) and sieved to obtain particles of under 0.5 mm. RS aqueous extract was obtained by ultrasound pre-treatment, followed by a heating reflux step (Freitas et al., 2020). A probe high-intensity ultrasonic homogeniser (Vibra CellTM VCX750, Sonics & Material, Inc., Newtown, CT, USA) was used to sonicate the RS: a distilled water suspension, with a ratio of 1:20 (m/v), at 25 ℃ (using an ice bath to prevent excessive heating) for 30 min, applying a frequency of 20 kHz, 750 W power, and 40% sonication amplitude. After that, the plant suspension was heated using a typical reflux device at 100 ℃ for 1 h. The RS extract was obtained by vacuum filtration using a vacuum pump (MZ 2 C NT, 7.0 mbar, Vacuubrand, Germany) with a Buncher funnel and qualitative filter (Filterlab). Then, the RS dry extract was obtained by freeze drying (Telstar, model LyoQuest-55) at − 60 ℃, 0.8 mbar for 72 h, and stored in a dark glass bottle at 4 ± 2 ℃ until further use. A total volume of about 750 mL of aqueous extract was freeze-dried in each cycle. The total solid yield obtained after freeze drying process was 14 g dried extract 0.100 g^{-1} RS.

2.3. Preparation of films

PLA pellets was initially conditioned in a desiccator containing P_2O_5 for 2 days to remove residual water. PLA films were obtained both with and without RS freeze-fried extract using PEG1000 (at 8% wt. with respect to the polymer mass), as plasticiser, by melt blending and compression moulding. As summarised in Table 1, the incorporation of the active extracts in the films was performed by adding percentages of 2%, 4%, and 6% wt. of RS extract (with respect to the total polymer mass) to the control mixture (PLA/PEG1000). The mixing process was performed in an internal mixer (HAAKE^{TM} PolyLab^{TM} QC, Thermo Fisher Scientific, Germany) at 160 ℃ and 50 rpm for 6 min. After cold milling the solid blend, the compression-moulding process was performed using a hydraulic press (Model LP20, Labtech Engineering, Thailand). To this end, 3 g of the pellets were put onto Teflon sheets and placed into the hydraulic press to obtain the films by preheating at 160 ℃ for 3 min, compressing at 160 ℃ and 100 bars for 3 min and final cooling for 5 min to 70 ℃.

2.4. Film characterisation

2.4.1. Microstructural properties

High resolution Field Emission Scanning Electron Microscopy (FESEM) was performed to study the structure of the film cross-sections. The films were cryo-fractured by immersion in liquid nitrogen, covered with platinum using an EM MED020 sputter coater (Leica BioSystems, Barcelona, Spain) and the images were taken with a Field Emission

Table 1
Mass fractions of the different formulations: PLA (0% wt. RS extract), PLARS2 (2% wt. RS extract), PLARS4 (4% wt. RS extract), PLARS6 (6% wt. RS extract).

Formulation	X_{PLA}	$X_{PEG1000}$	$X_{RS\ extract}$
PLA	0.926	0.074	–
PLARS2	0.909	0.073	0.018
PLARS4	0.893	0.071	0.036
PLARS6	0.877	0.070	0.053

Scanning Electron microscope equipped with focused ion gun (Auriga Compact, Zeiis, Oxford Instruments), at × 400 magnification (with inserts at ×2000), using an acceleration voltage of 2.0 kV.

2.4.2. 2.4.2 Optical properties

A spectro-colorimeter CM-3600d (Minolta Co. Tokyo, Japan) was used to measure the transparency by means of the internal transmittance (T_i) parameter. The Kubelka-Munk theory of multiple scattering, using the film reflection spectra obtained on black and white backgrounds, was used to find T_i at a light wavelength range of 400–700 nm. The measurements were taken six times for each formulation. A D65 illuminant and 10º observer were used to obtain the film's colour coordinates L^* (lightness), a^* (redness-greenness), and b^* (yellowness-blueness) from the infinite reflectance (Freitas et al., 2022).

The film's colour was analysed by means of the psychometric coordinates, Chroma or saturation (C^*) (Eq. 1), and hue angle (h^*) (Eq. 2):

$$C^* = \sqrt{a^{*2} + b^{*2}} \quad (1)$$

$$h^* = arctg\left(\frac{b^*}{a^*}\right) \quad (2)$$

The colour difference between the films containing extract and the extract-free film was also determined though the Total Colour Difference parameter (ΔE^*) (Eq. 3).

$$\Delta E^* = \sqrt{(\Delta L^*)^2 + (\Delta a^*)^2 + (\Delta b^*)^2} \quad (3)$$

Where ΔL^*, Δa^* and Δb^* correspond to the differences between the colour parameters of the active and the control films.

2.4.3. Mechanical properties

The thickness of the films was measured using a digital micrometer (Palmer, model COMECTA, Barcelona, accuracy of 0.001 mm) at ten random film positions.

Tensile strength (TS), elastic modulus (EM) and the elongation at break (EB) of the films were determined using a universal test machine (TA.XTplus model, Stable Micro Systems, Haslemere, England) following the standardised ASTM D882 method (ASTM, 2012). The control and active films were cut (2.5 ×10 cm), mounted in the film-extension grips of the testing machine and lengthened at a cross-head speed of 12.5 mm/min until breaking. Eight samples per formulation were evaluated.

2.4.4. Thermal behaviour

A thermogravimetric analyser (TGA 1 Star^e System, Mettler-Toledo Inc., Switzerland) was used to measure the thermal stability of the films. The samples (3–5 mg) were placed in an alumina crucible and heated in a single-step thermal program from 25 ℃ to 700 ℃ at a heating rate of 10 ℃.min^{-1} under a nitrogen flow (10 mL.min^{-1}). The derivative curves (DTGA) of the thermograms were obtained using the STAR^e Evaluation Software (Mettler-Toledo, Switzerland). The initial degradation temperature, the temperature at maximum degradation rate and the mass loss percentage in each detected thermal event were determined. The analysis was performed in triplicate for the extract, PEG1000 and PLA films.

Differential scanning calorimetry (DSC) analysis was performed in a differential scanning calorimeter (Star^e System, Mettler-Toledo Inc., Switzerland). The film samples (5–7 mg) were placed in aluminium-sealed pans and a five-step thermal program was performed under a nitrogen flow (30 mL.min^{-1}). The samples were heated from − 25–200 ℃ at a heating rate of 10 ℃.min^{-1}, maintained at 200 ℃ for 5 min, cooled down to − 10 ℃ at − 50 ℃.min^{-1}, maintained at − 10 ℃ for 5 min, and heated up again to 200 ℃ at a heating rate of 10 ℃.min^{-1}. The analysis was performed in triplicate for each film formulation.

2.4.5. Barrier properties

According to ASTM E96/E96M (ASTM, 2005), a gravimetric method, using the modification of Mchugh et al. (1993), was used to determine the water vapour permeability (WVP). The 3.5 cm diameter films were placed on Payne permeability cups (Elcometer SPRL, Hermelle/s Argenteau, Belgium) filled with 5 mL of distilled water (100% relative humidity) and sealed. The cups were placed in a desiccator at 25 ℃ with $Mg(NO_3)_2$ to maintain the relative humidity at 53%. A fan was placed on top of each cup to decrease the resistance to water vapour transport. The cups were weighed every 1.5 h for 25 h with an analytical balance (± 0.0001 g) and the WVP was calculated from the slope of the weight loss-time curves (Freitas et al., 2021). The analysis was performed in triplicate for each formulation.

The oxygen permeability (OP) was determined following a modified version of the ASTM,2010. Three replicates per formulation were measured using an OX-TRAN Model 2/21 mL (Mocon Lippke, Neuwied, Germany) at 25 °C and 53% of RH. The film samples (50 cm^2) were exposed to an oxygen flow and the oxygen transmission was obtained every 15 min until equilibrium was reached. The OP values were calculated by dividing the oxygen transmission by the difference in partial pressure of oxygen between the two sides of the film, and then multiplying by the average film thickness.

2.5. Antioxidant activity of the RS extract and films

The RS extract, and the amount of it released from the films into food simulants, were characterised as to the total phenolic content (TPC) and antioxidant activity. For this, an aqueous solution of freeze-dried extract was prepared at 2.5 mg.mL^{-1}. The TPC analysis was carried out in triplicate using a modified version of the Folin-Ciocalteu method (Menzel et al., 2020) and the results were expressed as mg gallic acid equivalent (mg GAE) per g of solid extract.

The antioxidant capacity of the dry RS extract was determined by using the DPPH (2,2-Diphenyl-1-pikryl-hydrazyl) radical scavenging method (Brand-Williams et al., 1995), with some modifications (Freitas et al., 2020). The antiradical activity was evaluated in triplicate by obtaining the EC_{50} parameter, defined as the amount of sample required to reduce the DPPH concentration by 50% when the reaction stability is reached.

2.6. Release kinetics of antioxidant compounds in food simulants

The release kinetics of the RS extract compounds from the films to different food simulants (A: ethanol 10% (v/v) and D1: ethanol 50% (v/v) was analysed following the methodology proposed by Requena et al. (2017), with some modifications. Approximately 2 g of control and active films were cut (1 ×1 cm squares) and immersed in the corresponding simulant at a ratio of 1:10 and maintained under stirring at 20 ℃ for 24, 72, 144 and 240 h. After each time, the liquid was filtered (Filter-Lab, 0.45 μm) and analysed as to TPC and the radical scavenging activity (EC_{50}), as described in Section 2.5. All of the experiments were carried out in duplicate. The EC_{50} values were referred per mass unit of extract incorporated into the film (mg of dry extract/mg DPPH).

Peleg's equation (Eq. 4) (Peleg, 1988) was used to model the release kinetics, in terms of percentage of phenolic content released with respect to the total content incorporated into the films (M_t), as a function of time. The initial release rate ($1/k_1$) and the maximum release ratio at equilibrium (EV: $1/k_2$) were obtained from model fitting. This was carried out by non-linear optimisation mode, using the solver tool from Excel.

$$M_t = \frac{t}{k_1 + k_2 t} \quad (4)$$

In order to elucidate the mass transfer mechanisms involved in the extract compound release into each food simulant, the Korsmeyer-Peppas model (Eq. 5) (Peppas & Peppas, 1994) was also fitted to the

experimental data.

$$\frac{Mt}{M\infty} = kt^n \quad (5)$$

Where M_t/M_∞ is the released ratio at time t with respect to the equilibrium value, k is the release rate constant, involving the diffusion coefficient, and *n* is the transport exponent related to the mass transfer mechanisms.

2.7. Statistical analysis

The statistical analysis was carried out using Minitab 17 Statistical Software. The analysis of variance (ANOVA) and Tukey's studentised range HSD (honestly significant difference) tests were used to check the significant differences between the film treatments, using the least significant difference (α) of 5%. Multifactorial regression models were fitted to describe the release of phenolic compounds and antioxidant activity in different food simulants, considering the extract concentration in PLA films and the contact time with the simulants and interactions between both factors. The goodness of fitted models was verified by the lack-of-fit test, the significance of the coefficients by the Student's t-test (α = 0.05), and the determination coefficient (R^2).

3. Results and discussion

3.1. Film characterisation

3.1.1. Microstructural properties

Fig. 1 shows the FESEM images of the cross section of the cryo-fractured PLA films incorporating or not the active extract at different concentrations. The control PLA film exhibited a smooth and homogeneous surface pattern, showing brittle and rubbery domains in the polymer matrix, as previously observed by other authors for similar PLA films (Muller et al., 2017b). The plastic fracture observed in the PLA film is characteristic of plasticised amorphous polymers, as previously observed by other authors (Hernández-García et al., 2021; Muller et al., 2017a). When the RS extract was incorporated into the films, small changes in the internal microstructure were revealed by their different cryo-fracture behaviour, which exhibited areas with a more brittle fracture, as observed by other authors when tannic acid was incorporated into starch-chitosan films (Talón et al., 2017). This suggests the possible establishment of interactions between some of the RS extract components and the PLA/PEG1000 matrix. Menzel et al. (2020) identified several phenolic compounds in the aqueous RS extract, such as *p*-coumaric, protocatechuic, ferulic, caffeic, vanilinic, tricine, and vanillin acids, which can establish hydrogen bonds with the carbonyl group of PLA chains (Fig. 2c). Moreover, as the extract concentration rose in the films, changes in the cross-section appearance were observed along with an increase in the surface roughness. The presence of non-miscible compounds within the polymer matrix produced small aggregates dispersed in the matrix, while both miscible and non-miscible compounds modified the film cryofracture pattern. These differences in the microstructural arrangement in the active films, compared with the control, could affect their physical properties.

3.1.2. Optical properties - Colour and internal transmittance of the active films

The visual appearance of the PLA films is shown in Fig. 2a. Observation with the naked eye showed no marked differences in the transparency of the films, whereas the colourless PLA films became more yellow-brown as the RS extract concentration increased, exhibiting small dot-like shapes with a slightly darker colour due to the dispersed solid fraction of the extract, more visible in the most concentrated films. The presence of the coloured compounds and small solid particles affected the colour properties of the samples: typically, the internal transmittance spectrum (T_i) (Fig. 2a) and the colour coordinates of the PLA films (Table 2).

T_i is closely related to the internal microstructure of the polymer matrix and the component arrangement, which will determine the degree of light scattering and the film transparency (Muller et al., 2017a). As shown in Fig. 2a, neat PLA films exhibited the highest transmittance

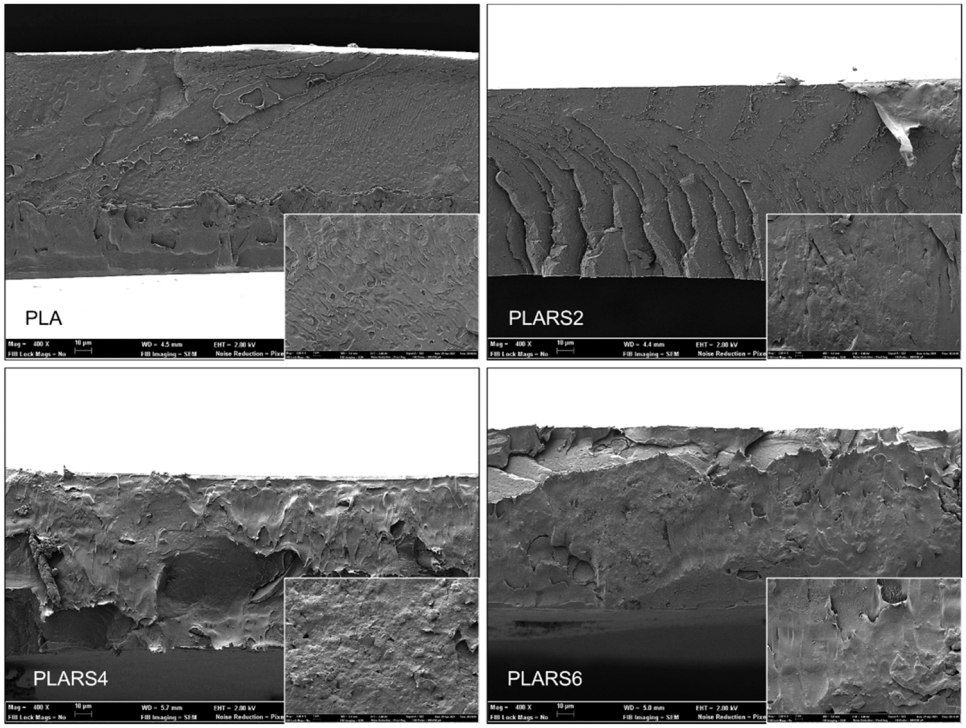

Fig. 1. FESEM images of the cross section of PLA films without extract and with different concentrations of RS extract: 2% wt. (PLARS2), 4% wt. (PLARS4), and 6% wt. (PLARS6).

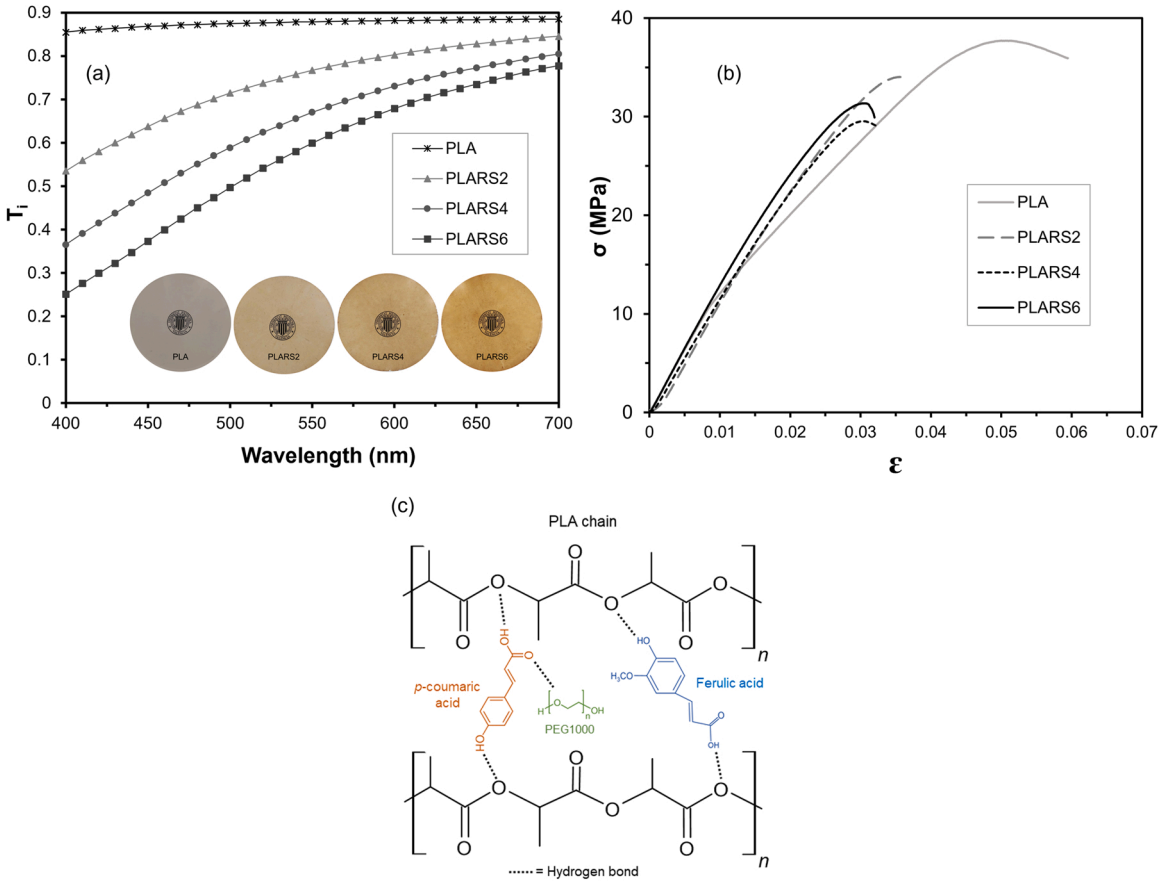

Fig. 2. (a) Visual appearance and internal transmittance spectra of films; (b) Stress-strain curves of PLA films with different RS extract concentrations (PLA: control; PLARS2: 2% wt.; PLARS4: 4% wt.; PLARS6: 6% wt.); (c) Possible hydrogen bonds among the phenolic compounds present in the RS extract and polymer chains.

Table 2
Optical properties of PLA-based films with different RS extract concentrations (0, 2, 4 or 6% wt.). L^*: luminosity; C^*: chroma; h^*: hue; ΔE^*: colour difference. Mean values and standard deviations.

Formulation	L^*	C^*	h^*	ΔE^*
PLA	90.7 ± 0.2^a	2.50 ± 0.13^a	99.6 ± 0.8^a	–
PLARS2	81.5 ± 0.4^b	18.31 ± 0.50^b	85.6 ± 0.2^b	18.4 ± 0.6
PLARS4	73.8 ± 0.3^c	27.31 ± 0.26^c	80.5 ± 0.1^c	30.1 ± 0.4
PLARS6	67.6 ± 0.7^d	34.70 ± 0.65^d	77.1 ± 0.3^d	39.7 ± 0.6

Different letters in the same column indicate significant differences between films by the Tukey test ($\alpha = 0.05$).

values, in coherence with the high film transparency and homogeneity. A gradual decrease in the T_i values was observed when the concentration of the extract rose, in agreement with that observed by other authors when plant extracts were incorporated into polymer matrices (Collazo-Bigliardi et al., 2019; Freitas et al., 2020). Differences in the T_i values must be attributed to the selective light absorption of the incorporated coloured compounds as well as to the light scattering effect provoked by non-miscible particles in the matrix, thus reducing the light transmission at the corresponding wavelengths.

Table 2 shows the values of colour coordinates for the different films, lightness (L^*), Chroma (C^*), hue angle (h^*) and the total colour difference (ΔE^*) with respect to the extract free PLA film. The L^* and h^* values progressively decreased ($p < 0.05$) as the RS extract rose in the film, whereas the Chroma and total colour difference (ΔE^*) significantly increased. This agrees with the fact that the extract made the films darker and more saturated in a reddish colouration. Menzel et al. (2019) also observed this tendency when incorporating aqueous extracts from sunflower hulls into starch-based films.

3.1.3. Mechanical properties

Fig. 2b shows the typical stress-strain curves of PLA films with and without differing ratios of RS extract. From the curves, the film's mechanical parameters, namely elastic modulus (EM), tensile strength at break (TS), and elongation at break (E%), were obtained and shown in Table 3. As can be observed in Fig. 2b, the samples exhibited the typical plastic behaviour, where the most resistant and stretchable sample prior

Table 3
Thicknesses, tensile properties (TS, E%, EM), oxygen permeability (OP), and water vapour permeability (WVP) of PLA films containing different RS extract concentrations (PLA: control; PLARS2: 2% wt.; PLARS4: 4% wt.; PLARS6: 6% wt.). Mean values and standard deviations.

Formulation	Thickness (mm)	E (%)	TS (MPa)	EM (MPa)	OP $x10^{18}$ ($m^3.m.m^{-2}.s^{-1}.Pa^{-1}$)	WVP $x10^{14}$ ($kg.m.Pa^{-1}.s^{-1}.m^{-2}$)
PLA	0.146 ± 0.009^a	6.0 ± 0.7^a	34 ± 3^a	1255 ± 36^{ab}	1.66 ± 0.01^a	3.14 ± 0.19^c
PLARS2	0.148 ± 0.006^a	3.4 ± 0.2^b	34.0 ± 1.4^a	1288 ± 34^{ab}	1.56 ± 0.04^a	3.55 ± 0.13^{bc}
PLARS4	0.145 ± 0.007^a	3.4 ± 0.3^b	29 ± 3^b	1232 ± 25^b	1.56 ± 0.03^a	4.00 ± 0.05^{ab}
PLARS6	0.142 ± 0.006^a	3.1 ± 0.2^b	30.7 ± 2.2^b	1315 ± 76^a	1.54 ± 0.06^a	4.21 ± 0.39^a

* E%: elongation at break; TS: tensile strength at break; EM: elastic modulus. Different letters in the same column indicate significant differences between films by the Tukey test ($\alpha = 0.05$).

to fracture was the control film without a RS extract. These mechanical parameters slightly worsened in active films, which became more brittle (less extensible with lower resistance to break). This indicates that the compounds of the RS extract modify the chain interactions in the polymer matrix, regardless of their concentration. Table 3 summarises the values of E%, TS and EM obtained for the different film formulations as well as their thickness. The thicknesses of the different films were not significantly different ($p < 0.05$), having an average value of 0.145 mm, in the range of those obtained by Muller et al. (2017b) for the same polymer and process conditions. The addition of the active extract in the polymer matrix provoked a decrease in the E% values of the films ($p < 0.05$), regardless of the extract concentration used. Thus, the active films were less stretchable (about 43%) than the control film. This effect was also observed by Jamshidian et al. (2012a) for antioxidant PLA-based films with ascorbyl palmitate and can be attributed to several factors. The potential hydrogen bonds established between the extract phenolic compounds (Fig. 2c) and both PEG1000 and PLA chains could reduce the polymer matrix stretchability, while the inter-chain forces could be reduced by the interruptions caused by the presence of other molecules/particles, thus giving rise to less resistant and more brittle matrices. Non-significant differences in the TS values ($p > 0.05$) were observed when up to 2% of the extract was incorporated, while higher concentrations provoked a slight decrease (about 13%), leading to less resistant films. The interactions between the extract compounds and PLA and PEG1000 chains and the small, dispersed particles could reduce the cohesion forces in the polymer matrix due to steric hindrance for inter-chain forces. The presence of the small particles (compound aggregates) within the polymer matrix, as observed in the FESEM micrographs (Fig. 1), could act as stress concentrators, thus decreasing the TS values. Similar results were found by Vilarinho et al. (2021) when incorporating green tea extract into PLA films reinforced with cellulose nanocrystals. In contrast, no notable differences were found between the EM values of the active and control films.

3.1.4. Barrier properties – Water vapour and oxygen permeability

The WVP and OP values of the different PLA films are summarised in Table 3. The extract-free PLA film exhibited WVP and OP values of 3.14×10^{-14} kg.m.Pa^{-1}.s^{-1}.m^{-2} and 1.66×10^{-18} m^3.m.m^{-2}.s^{-1}. Pa^{-1}, respectively, similar to those found in previous studies (Hosseini et al., 2016; Muller et al., 2017b). The incorporation of the RS extract slightly decreased the barrier capacity of the films to both water vapour and oxygen, although the OP values were not significantly affected. This can be attributed to the decrease in the matrix cohesion forces provoked by the extract, as deduced from the mechanical behaviour. The hydrophilic nature of the RS extract could also contribute to the lower water vapour barrier capacity of the films, promoting the film's water affinity and the permeation of water molecules. Other studies also reported higher WVP values in PLA-based films with bioactive compounds (Vilarinho et al., 2021; Roy & Rhim, 2020; Srisa & Harnkarnsujarit, 2020). Nevertheless, despite the slight worsening in their water vapour barrier capacity, the films incorporating bioactive extracts present interesting properties with the potential to protect packaged foods from oxidation and microbial spoilage.

3.1.5. Thermal behaviour

Fig. 3(a and b) shows the TGA curves and their derivatives (DTGA), obtained for the different films and RS extract and Table 4 summarises the parameters of the thermal degradation events detected for each film

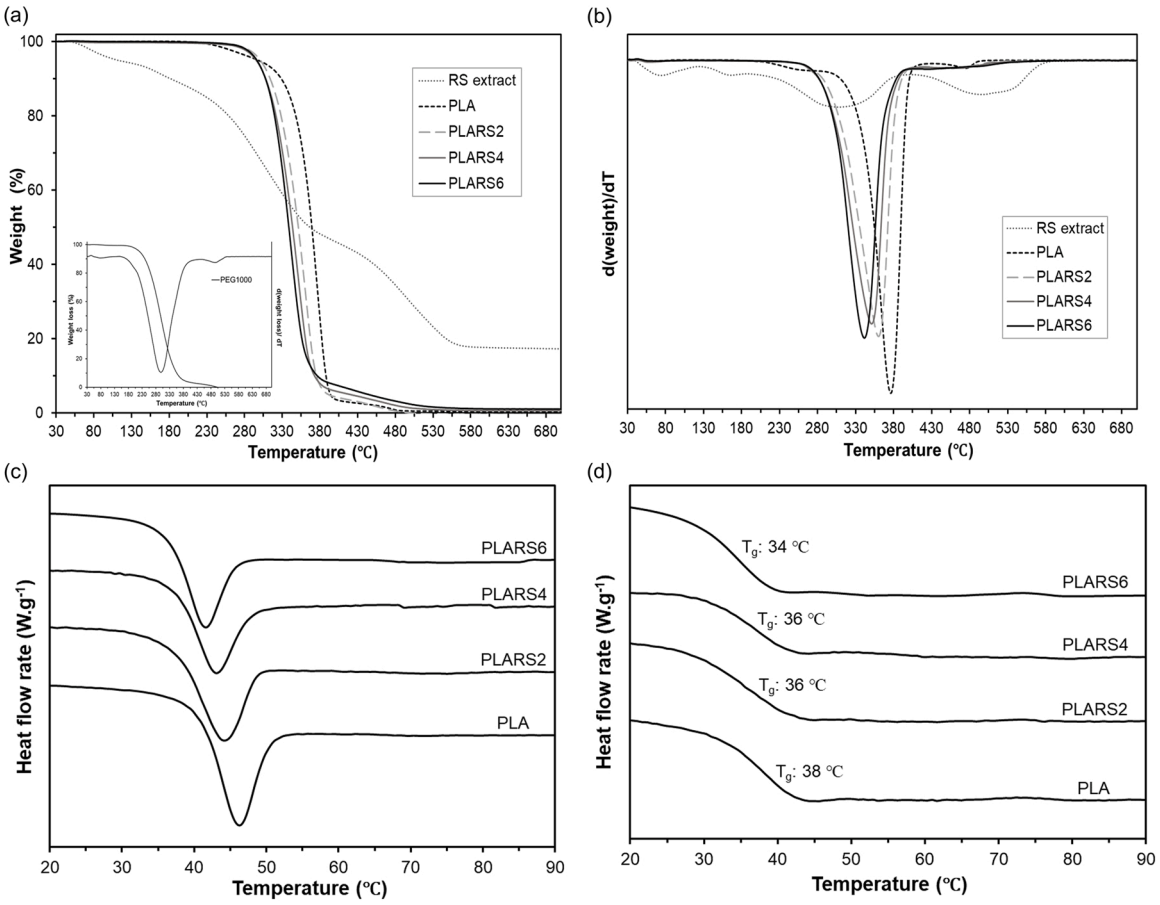

Fig. 3. TGA curves (a), DTGA derivative curves (b), and DSC (c: first heating, d: second heating) thermograms of PLA films with different RS extract concentrations (PLA: control; PLARS2: 2%; PLARS4: 4%; PLARS6: 6%).

Table 4
Thermal degradation parameters (onset (T_o), end (T_e), and peak (T_p) temperatures, mass loss (ΔM), and residual mass) of the films and DSC parameters (relaxation enthalpy -ΔH_{relax}- from the first heating scan, and glass transition temperature (T_g) from the second heating scan). (PLA: control; PLARS2: 2% extract.; PLARS4: 4% extract.; PLARS6: 6% extract).

	TGA					DSC	
Formulation	**T_o (℃)**	**T_e (℃)**	**T_p (℃)**	**Δm (%)**	**Residue (%)**	**ΔH_{relax} (J/g)**	**T_g**
PLA	190 ± 6^{b}	495 ± 1^{a}	376 ± 1^{a}	97.3 ± 0.1^{a}	0.4 ± 0.2^{a}	5.4 ± 0.1^{a}	38 ± 3^{a}
PLARS2	237 ± 2^{a}	511 ± 1^{b}	361 ± 2^{b}	96.4 ± 0.2^{b}	0.5 ± 0.1^{a}	4.3 ± 0.8^{ab}	36 ± 2^{a}
PLARS4	239 ± 4^{a}	535 ± 4^{c}	351 ± 1^{c}	94.2 ± 0.1^{c}	0.6 ± 0.6^{a}	3.1 ± 0.1^{b}	36 ± 2^{a}
PLARS6	234 ± 1^{a}	566 ± 3^{d}	342 ± 1^{d}	98.5 ± 0.2^{d}	1.1 ± 0.3^{a}	3.4 ± 0.1^{b}	34 ± 2^{a}

Different letters in the same column indicate significant differences between films by the Tukey test ($\alpha = 0.05$).

formulation: onset (T_o), peak (T_p) and end temperature (T_f), percentage of mass variation (Δm) and residual mass. The thermal degradation of the RS extract was also analysed to better understand its behaviour during the film thermoprocessing and its potential effect on the thermal behaviour of PLA films. As shown in Fig. 3(a and b), the RS extract showed several thermodegradation steps, coherently with its complex composition: a first step, between 45 and 130 ℃, that can be mainly attributed to water loss (mass loss of around 6%) and several steps above 130 ℃, which can be attributed to the degradation of the different components present in the extract. These results suggested that a fraction of the extract is likely degraded during the film manufacturing process (160 ℃) in agreement with that reported by other authors (Menzel et al., 2019). The great residual mass of the extract (around 20%) suggested that it contains a high percentage of silica and other minerals from RS (Chen, 2011).

As concerns the TGA analysis of the films (Fig. 3a), all of the samples exhibited a single degradation step starting at about 190 ℃ in the extract-free PLA and 235 ℃ in films with the RS extract, with a total mass loss of over 95–98%. The temperature at which the maximum degradation rate may be found (T_p in Table 4) is significantly reduced when the RS extract is present in the films. This indicates that the RS extract compounds affect the thermodegradation of PLA, which could be attributed to their interference with the interchain forces affecting the matrix cohesion and compactness, as deduced from the tensile and barrier properties. Likewise, the presence of several types of phenolic acids in the RS extract (Menzel et al., 2020; Elzaawely et al., 2017) could favour the partial hydrolysis of PLA into low molecular weight compounds, thermally less stable, thus lowering the degradation temperatures. In contrast, the thermal degradation of the extract-free PLA film started earlier (lower T_o) than the films with the RS extract (Fig. 3b). This could be attributed to the initial thermal degradation of the plasticiser PEG1000 (T_o: 160 ℃, T_p: 300 ℃), as observed in its TGA and DTGA curves embedded into Fig. 3a, which seems not to occur in films containing the RS extract. This suggests that PEG could also interact with the extract components, promoting its thermal stability and delaying its degradation at higher temperatures. There was no significant difference in the residual mass of the films (< 1%) despite the different RS extract concentration with notable residual mass. This can be explained by the relatively low amount of RS extract present in every formulation, which not significantly affect the overall residue of the films.

The glass transition temperature (T_g) of the PLA in every film was analysed by DSC. Thermograms of the first and second heating scans of the different films are shown in Figs. 3c and 3d, respectively, where the relaxation endotherms, associated with the ageing of the polymer, can be observed in the first scan in the glass transition region. Table 4 shows the values of T_g obtained from the second heating scan, where thermal history is erased, and the relaxation enthalpy obtained from the first heating scan. The PLA control film showed a T_g value of 37.7 ℃, similar to that reported by other authors for PEG 1000 plasticised amorphous PLA (Muller et al., 2017b). The T_g values of active films tended to decrease slightly when the RS extract rose in the films, although the differences were not statistically significant. Likewise, as the extract concentration increased, the polymer relaxation enthalpy (expressed per gram of polymer) significantly decreased ($p < 0.05$), which suggests that extract compounds also inhibited the degree of PLA chain reassociation during ageing to some extent.

Therefore, the incorporation of the RS extract into PLA films, at the concentration levels used, partially limits the interchain forces in the PLA matrix, making the polymer matrix slightly less cohesive, as reflected in the decrease in the film's mechanical resistance, extensibility and barrier capacity, and the small changes in the thermal behaviour. Nevertheless, the observed changes were no remarkable to compromise the food packaging requirements of films, including thermal, barrier, and mechanical performance. In this sense, besides exhibiting suitable functionality for packaging purposes, the potential antioxidant capacity of the films can be considered an important improvement for food preservation purposes.

3.2. Antioxidant properties of the PLA films containing RS extract

The antioxidant capacity of the films was analysed through the release study of potentially active compounds of RS extracts into food simulants of differing polarities that can emulate foods systems with different fat contents (Requena et al., 2017). The antioxidant capacity of the RS extract was first analysed through its TPC and DPPH radical scavenging capacity. Afterwards, these activities were analysed in the simulants in contact with the films for different times, where differing extents of the potentially active compounds were released.

3.2.1. Content of phenolic compounds and DPPH radical scavenging capacity of RS

The RS extract obtained via aqueous extraction by reflux heating for 1 h after 30 min US pre-treatment was selected on the basis of a previous study where these conditions gave rise to a phenolic-rich extract with high DPPH radical scavenging capacity (Freitas et al., 2020). The value of TPC obtained in the dry extract was 37.1 ± 0.4 mg GAE/g. This value is higher than that obtained by Menzel et al. (2020) in rice straw, using aqueous extraction at room temperature (29 mg GAE/g dry extract). These authors reported that the most abundant phenolic compounds analysed in the rice straw extract were ferulic, protocatechuic and *p*-coumaric acids.

As concerns the DPPH radical scavenging capacity of the RS extract, the EC_{50} value obtained was 6.3 ± 0.3 mg freeze-dried extract/mg DPPH, in agreement with that previously reported for the same extraction conditions (Freitas et al., 2020). This value was a great deal lower (greater antioxidant activity) than that found by Menzel et al. (2020) for the RS extracts obtained at room temperature using water, methanol and ethanol as solvents (12, 20 and 19 mg freeze-dried extract/mg DPPH, respectively). This indicates that the use of US and high temperatures in water extraction promoted the release of highly antioxidant phenolic compounds with potential applications as food antioxidants. Ultrasound provokes an increase in the contact points between the RS matrix and the solvent, caused by collisions between the particles and the shock waves created by the collapse of cavitation bubbles in the liquid, consequently increasing the solid transfer from the RS to the solvent

(Cheung & Wu, 2013; Hayat et al., 2019). Furthermore, when heat treatment is applied, the plant tissue becomes softened, which reduces its integrity and weakens the bonds between phenolics and the plant matrix, enhancing the extraction yield. Indeed, Li et al. (2015) stated that extracting phenolic compounds from a plant matrix is achieved when there is a disruption of the ester and ether bonds between the analyte and the lignocellulosic fraction.

3.2.2. *Release kinetics of antioxidant compounds into food simulants*

The release of these active compounds is needed for them to exert the protective action in the target substrate. The analyses of TPC and antioxidant capacity at different times of film immersion in two food simulants (A: 10% ethanol, and D1: 50% ethanol) would permit the prediction of the antioxidant capacity of the different films when applied as packaging systems on different foods. Fig. 4 shows the percentage of TPC released in both simulants, with respect to the TPC present in the film with the incorporated RS extract. As expected, the total amount of released phenolic increased as the contact times lengthened and it was higher when the extract concentration in the films rose, according to the higher driving force for mass transfer (greater concentration gradient). The release pattern was also affected by the type of simulant. Thus, the phenolic compounds were released faster and at a higher ratio into simulant D1, whereas in the more polar simulant A, the process was more limited, almost reaching a plateau level after 2 contact days, with a very low percentage of compounds released, especially in the case of the films with the lowest extract ratio. In contrast, simulant D1 (50% ethanol) favoured the release of greater amounts of phenolic compounds, with scarcely any differences between films with differing extract ratios. This variation in release behaviour is coherent with that observed by other authors analysing the release behaviour of different antioxidants from PLA, which was greatly promoted by the ethanol ratio in the food simulant (Jamshidian et al., 2012b). The compound's chemical affinity with the polymer matrix and its solubility in the simulant define the partition coefficient at equilibrium. In this sense, the main phenolic compounds of aqueous RS extract, as determined by Menzel et al. (2020) are ferulic, *p*-coumaric and protocatechuic acids, which are more soluble in ethanol than in water. Thus, the increase of ethanol ratio in the simulant will promote the solubility of these phenolic acids. It is worth mentioning that the nature of the phenolic compounds released in each simulant could be different, being the phenolic compounds released in simulant A more polar than in simulant D1. Likewise, the distinct profiles of phenolic compounds released would lead to different bioactivity of the material due to both the total amount and nature of the released compounds. In addition to the differences in compound solubility, changes in the polymer matrix in contact with the liquid phase also affected the release behaviour. Thus, the higher ethanol ratio of simulant D1 permitted the penetration of ethanol into the matrix, provoking swelling and the relaxation of the hydrophobic PLA matrix (Sato et al., 2013), which could favour the release of the compound into the simulant, attaining higher percentages of released phenolics. In contrast, the high polarity of simulant A (10% ethanol) makes it difficult for the hydrophobic film to swell, leading to reduced release rates.

The parameters obtained by fitting the Peleg's equation are shown in Table 5, where the values of the determination coefficient (R^2) were also included. As expected, the initial release rate ($1/k_1$) increased when the extract concentration rose in the film and was similar for 4% and 6% of extract in both simulants. The lowest release rate was obtained for films with 2% of RS extract, especially in simulant A. The equilibrium values (EV=1/k2) in simulant A also increased when the extract concentration rose (9–33% release), whereas a complete release was estimated at infinite time (EV value) in simulant D1. In fact, this value must be limited to 100% in the optimisation process of the model parameters. The obtained results point to an enhancement in both the release ratio and rate when the extract concentration was higher than 2%, which can also be attributed to the more open PLA matrix (weaker interchain forces) promoted by the presence of higher extract ratio in the matrix.

The parameters obtained by fitting the Korsmeyer-Peppas model in each food simulant, are also shown in Table 5. The values of n coefficient were equal to or lower than 0.5 for data obtained in simulant A, thus indicating that Fickian or quasi-Fickian diffusion mechanisms are involved in the release of the phenolic compounds from the PLA matrix. Nevertheless, films in the simulant that is richer in ethanol (D1) exhibited n values of over 0.5, attributed to anomalous transport where the compound diffusion is coupled with the polymer relaxation brought about by the effect of the solvent (Peppas & Brannon-Peppas, 1994). This confirms the hypothesised role of ethanol penetrating and swelling the PLA matrix, thus favouring the mass transfer rate by an anomalous mass transport mechanism where the polymer relaxation enhances the compound diffusion. Additionally, the hydrolytic degradation of the PLA matrix in the presence of ethanol has been described by other authors (Iñiguez-Sancho et al., 2016), which will also contribute to the promotion of mass transfer processes. This hydrolysis has been found to be much faster in 50% ethanol-aqueous solutions than in 95% ethanol or pure water. The creation of free volume due to the penetration of ethanol provoked the polymer swelling, thus allowing for more water

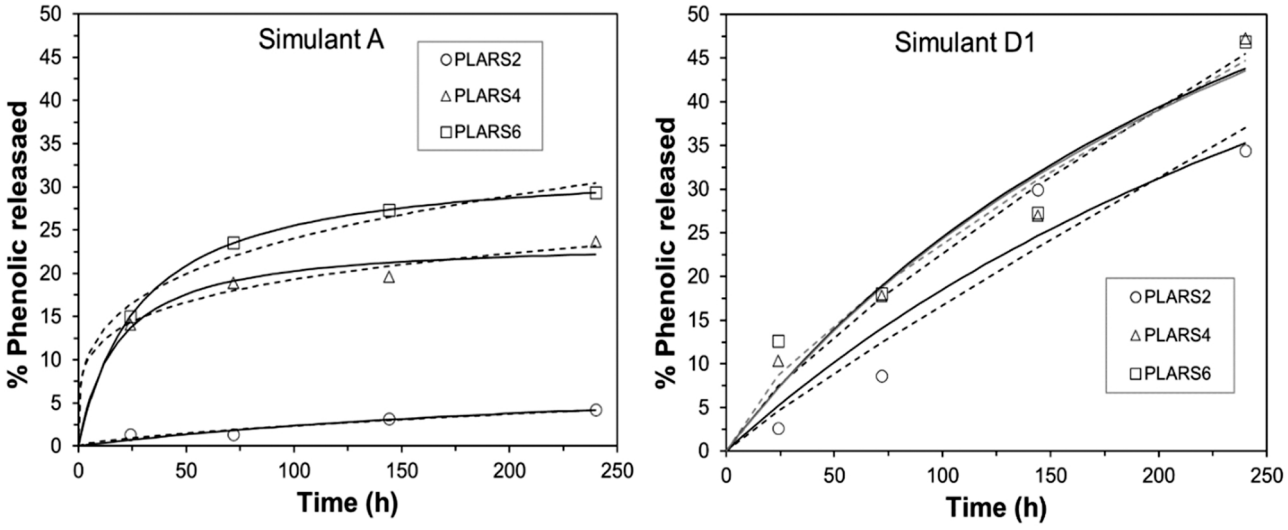

Fig. 4. Percentage of total phenolic released from active films as a function of time for simulants A and D: experimental data (points) and the Peleg (continuous lines) and Korsmeyer-Peppas (dashed lines) fitted models.

Table 5
Parameters of the Peleg and Korsmeyer-Peppas models obtained for simulants A (10% ethanol aqueous solution) and D1: (50% ethanol aqueous solution) for the films with differing concentrations of RS extract.

	Simulant A			Simulant D1			Simulant A			Simulant D1		
Treatment	k_1	EV	R^2	k_1	EV	R^2	n	k	R^2	n	k	R^2
PLARS2	31.5	9.4	0.936	4.4	100	0.937	0.66	0.012	0.950	0.91	0.003	0.933
PLARS4	0.74	23.9	0.985	3.1	100	0.964	0.21	0.307	0.992	0.79	0.006	0.982
PLARS6	0.86	32.8	0.999	3.1	100	0.951	0.27	0.212	0.989	0.71	0.009	0.971

molecules to diffuse into the PLA matrix, which accelerates the polymer hydrolysis rate up to 3.7 times in comparison with pure water (Tsuji, 2010; Iñiguez-Sancho et al., 2016). Nevertheless, all the films maintained their physical integrity throughout the entire experiment, despite changing their appearance, depending on the PLA matrix alteration.

Therefore, the different chemical interactions of the extract compounds with the PLA matrix and the degree of relaxation of the polymeric matrix in contact with the solvent affected the release kinetic parameters. Thus, the amount released at equilibrium was higher in simulant D1, which contains a higher proportion of ethanol, as also observed by other authors (Jamshidian et al., 2012b) studying PLA films containing different antioxidants. So, the maximum percentage of phenolic released was found in simulant D1 for films with higher extract concentrations. In real food systems, different food-PLA interactions could be expected, which would also affect the compound's release and the antioxidant's effectiveness.

The antioxidant capacity of the films was also analysed through the EC_{50} parameter. This indicates the DPPH radical scavenging capacity of the films, representing the amount of sample required to reduce the DPPH concentration by 50% when the reaction stability is reached; so, the lower the value, the higher the radical scavenging capacity. To compare the EC_{50} values obtained at different contact times in both simulants with the value of pure extract, the EC_{50} was expressed as equivalent mg extract/mg DPPH, considering the amount of extract incorporated in each film. Fig. 5 shows the EC_{50} values of the films vs. contact time, where the progressive decrease in EC_{50} was obtained as the release progressed. Therefore, the radical scavenging capacity increased in line with the release of the extract compound; however, in no case did the values reach those of the pure extract, always showing higher EC_{50} values (Fig. 5). However, as the contact time lengthened in simulant A, the films with 6% extract exhibited similar EC_{50} values to the films in simulant D1, in the range of 15 mg extract/mg DPPH. In contrast, the films with 2% and 4% of extract in simulant A reached asymptotic values of about 30 mg extract/mg DPPH, which even rose at final times when

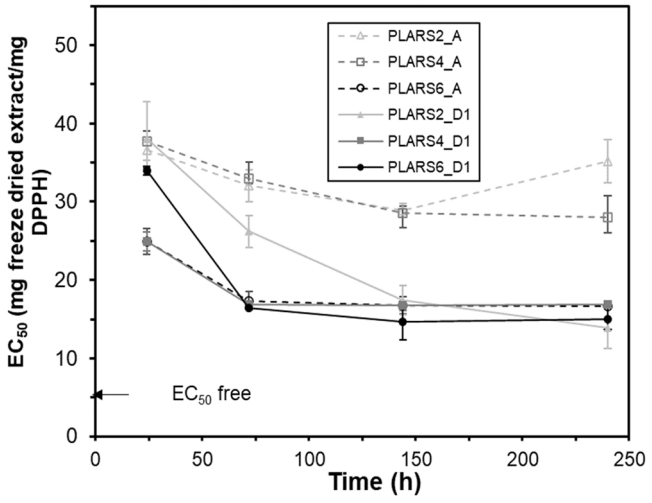

Fig. 5. EC_{50} values for the active films in simulants A and D1 over time. An arrow in the bottom right-hand corner of the graph shows the value of EC_{50} for the free extract (6.3 ± 0.3 mg dry extract/ mg DPPH).

the extract content was 2%, probably due to the oxidative degradation of the released compounds. Therefore, the radical scavenging capacity of the films with 6% RS extract was similar at relatively short contact times (150 h), regardless of the type of substrate in contact. The obtained results indicate that the compounds responsible for the radical scavenging capacity were not completely released from the films or were partially degraded during thermal processing, although there was notable activity (EC_{50} = 12 mg incorporated extract/mg DPPH) after about 150 h contact time in different simulated food systems when the films contained 6% of extract. Differences in the amount of phenolic compounds released did not explain the almost constant radical scavenging capacity, which suggests that this capacity was not only related with the total phenolic compounds estimated by the Folin-Ciocalteu method. For comparison purposes, the EC_{50} values of typical strong antioxidants, such as ascorbic acid or α-tocopherol, are 0.12 and 0.26 mg compound /mg DPPH, respectively (Brand-Williams et al., 1995).

3.2.3. Surface response for the antioxidant capacity of the films

In order to obtain a practical model that allows for estimating the released phenolic ratio and the radical scavenging capacity (EC_{50}) as a function of both contact time and extract concentration in the film, multifactorial regression models were also obtained, and the corresponding surface response (Fig. 6). The regression Eqs. 6 and 7 explained 98% and 93% of the variation in %GAE for simulants A and D1, respectively. Likewise, the radical scavenging capacity of the released compounds (EC_{50} parameter), expressed as mg film/mg DPPH were described by Eqs. 8 and 9, explaining 97% and 91%, respectively, in A and D1 simulants, of total EC_{50} variation.

$$\hat{Y}_{\%GAE}(Simulant\ \ A) = 0.040t - 0.0002t^2 + 15.745x - 1.478x^2 + 0.011xt - 26.87 \quad (6)$$

$$R^2 = 0.98$$

$$\hat{Y}_{\%GAE}(Simulant\ \ D1) = 0.162t + 7.940x - 0.763x^2 - 13.340 \quad (7)$$

$$R^2 = 0.93$$

$$\hat{Y}_{EC50}(Simulant\ \ A) = -6.030t - 0.020t^2 - 768.7x + 50.30x^2 + 3459 \quad (8)$$

$$R^2 = 0.97$$

$$\hat{Y}_{EC50}(Simulant\ \ D1) = -13.780t - 0.023t^2 - 1015x + 80.10x^2 + 1.241xt + 3889 \quad (9)$$

$$R^2 = 0.91$$

Fig. 6 clearly shows that, from 150 h contact time onwards, the films with the highest extract concentration in simulant A exhibited antioxidant capacity similar to that in contact with simulant D1, as commented on above. This indicates that, despite the greater release of total phenolics in simulant D1, the phenolics released in simulant A exhibited high antioxidant potential; the greater the amount of extract incorporated into the polymer matrix, the greater the degree of similarity between the antioxidant potential of the films in both simulants.

The maximum release of phenolic compounds and the minimum

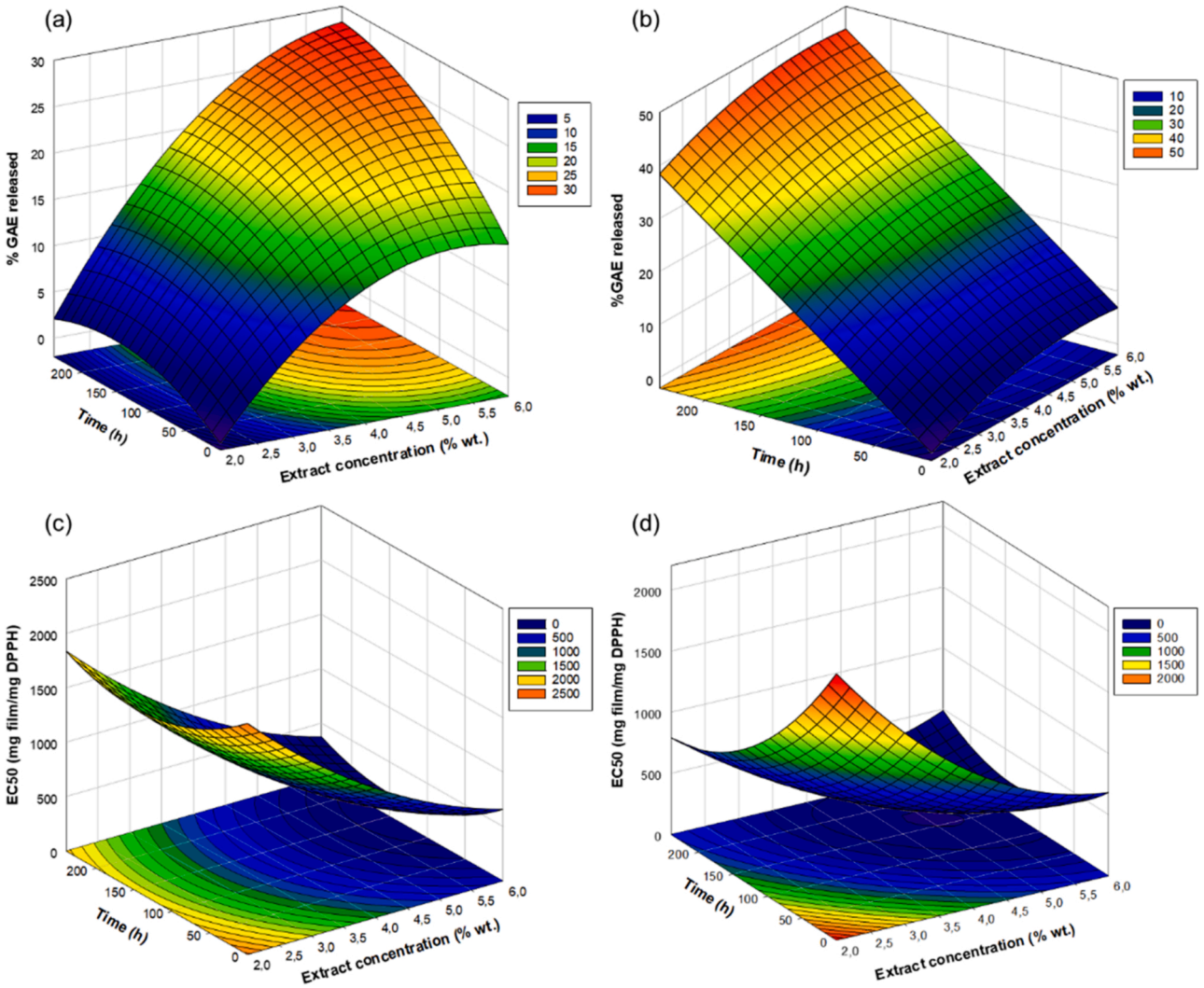

Fig. 6. Response surface plots from the fitted regression models for %GAE released in simulant A (a) and D1 (b), and EC_{50} of the PLA films in the simulants A (c) and D1 (d).

value of EC_{50} (maximum radical scavenging capacity) were obtained from the obtained functions. Thus, in simulant A, the optimal film formulation was that containing 6% wt. extract, with a maximum phenolic release of 30.4% of GAE at the final time (240 h), exhibiting the maximum radical scavenging capacity (EC_{50} = 209 mg film/ mg DPPH) at 148 h contact time. In simulant D1, the optimal films would contain 5.1% extract, which released 46.1% GAE at the final time (240 h), exhibiting the maximum radical scavenging capacity (EC_{50} = 201 mg film/mg DPPH) at 159 h contact time. Therefore, films with an extract concentration of nearly 6% exhibited a very similar radical scavenging capacity in both simulants after approximately 150 h contact time; this suggests that this extract concentration in the films ensures their potential antioxidant capacity in food systems regardless of their polar nature, despite the fact that the release of phenolic compounds would be greater in less polar substrates. To sum up, both time and extract concentration in the film affected the amount of phenolic compounds released and the potential radical scavenging capacity of films, but the latter reached an almost constant value from about 150 h contact time onwards for films with an extract concentration of nearly 6%. So, these PLA films could be used as biodegradable active packaging materials with antioxidant capacity in both aqueous foods (simulant A) or more fatty foods, such as oil-in water emulsions (simulant D1).

4. Conclusion

The rice straw aqueous extract obtained by an ultrasound-assisted and reflux-heating process had remarkable phenolic content and radical scavenging capacity. Its incorporation into PLA films turned them a little brown while slightly modifying the polymer chain arrangement and strength of the matrix, which promoted a small loss in the film stretchability, resistance to break, barrier capacity and PLA thermostability. However, the films gained antioxidant capacity when the extract was incorporated. The phenolic components incorporated into the extract were able to be released, depending on the extract concentration in the films, the food simulant polarity and contact time. In the ethanol-rich simulant (D1), the total content of phenolics could be released at equilibrium, whereas only 33% at most could be released in the most aqueous simulant (A). The radical scavenging capacity of the films, referred per mass unit of incorporated dry extract, reach asymptotic values from about 150 h contact time onwards; these were lower than those of the pure extract, but films with an extract concentration of nearly 6% exhibited very similar values in both simulants. This suggests

that this extract concentration in the films ensures their potential antioxidant capacity in food systems regardless of their polar nature. No good correlation between the amount of phenolic compounds released and the radical scavenging capacity was found, which suggests that other extract compounds contributed to this capacity of the films. So, PLA films incorporating about 6% of rice straw extract could be used as biodegradable active packaging material with interesting antioxidant capacity in both aqueous foods (simulant A) and more fatty products, such as oil-in water emulsions (simulant D1). Further studies will be carried out to verify their potential antioxidant efficiency in different real food systems.

Funding

This work was supported by the Agencia Estatal de Investi gación through project PID2019-105207RB-I00/AEI/10.13039/501100011033 and by Generalitat Valenciana [grant number GrisoliaP/2019/115]. Funding for open access charge: CRUE-Universitat Politècnica de València.

CRediT authorship contribution statement

Pedro A. V. Freitas: Conceptualization, Methodology, Formal analysis, Investigation, Writing – original draft, Writing – review & editing. **Nuria Julia Bas Gil:** Conceptualization, Methodology, Formal analysis, Investigation, Writing – original draft, Writing – review & editing. **Chelo González-Martínez:** Conceptualization, Methodology, Formal analysis, Investigation, Writing – original draft, Writing – review & editing. **Amparo Chiralt:** Conceptualization, Methodology, Formal analysis, Investigation, Writing – original draft, Writing – review & editing.

Conflict of interest

The authors have no conflict of interest to declare.

Data Availability

The authors do not have permission to share data.

Acknowledgments

The authors thank the Agencia Estatal de Investigación (Spain) for the financial support through projects PID2019–105207RB-I00/AEI/10.13039/501100011033 and Generalitat Valenciana [grant number GrisoliaP/2019/115].

References

ASTM. (2005). E96/E96M-05. standard test methods for water vapor transmission of materials. *American Society for Testing and Materials* (pp. 1–11).

ASTM. (2010). D3985-05 oxygen gas transmission rate through plastic film and sheeting using a coulometric sensor. *Annual Book of ASTM Standards C*, 1–7. https://doi.org/10.1520/D3985-05.2

ASTM. (2012). ASTM D882-12 standard test method for tensile properties of thin plastic sheeting. *American Society for Testing and Materials* (p. 12).

Arun, K. B., Madhavan, A., Sindhu, R., Binod, P., Pandey, A., Reshmy, R., & Sirohi, R. (2020). Remodeling agro-industrial and food wastes into value added bioactives and biopolymers. *Industrial Crops and Products, 154*, Article 112621.

Avérous, L., Fringant, C., & Moro, L. (2001). Plasticized starch–cellulose interactions in polysaccharide composites. *Polymer, 42*(15), 6565–6572. https://doi.org/10.1016/S0032-3861(01)00125-2

Balaji, A. B., Pakalapati, H., Khalid, M., Walvekar, R., & Siddiqui, H. (2018). Natural and synthetic biocompatible and biodegradable polymers. *Biodegradable and biocompatible polymer composites* (pp. 3–32). Elsevier. https://doi.org/10.1016/B978-0-08-100970-3.00001-8

Barana, D., Salanti, A., Orlandi, M., Ali, D. S., & Zoia, L. (2016). Biorefinery process for the simultaneous recovery of lignin, hemicelluloses, cellulose nanocrystals and silica from rice husk and Arundo donax. *Industrial Crops and Products, 86*, 31–39. https://doi.org/10.1016/j.indcrop.2016.03.029

Bassani, A., Montes, S., Jubete, E., Jesus, P., Sanjuán, A. P., & Spigno, G. (2019). Incorporation of waste orange peels extracts into PLA films. *Chemical Engineering Transactions, 74*, 1063–1068. https://doi.org/10.3303/CET1974178

Botterweck, A. A. M., Verhagen, H., Goldbohm, R. A., Kleinjans, J., & van den Brandt, P. A. (2000). Intake of butylated hydroxyanisole and butylated hydroxytoluene and stomach cancer risk: Results from analyses in the Netherlands Cohort Study. *Food and Chemical Toxicology, 38*(7), 599–605. https://doi.org/10.1016/S0278-6915(00)00042-9

Brand-Williams, W., Cuvelier, M. E., & Berset, C. (1995). Use of a free radical method to evaluate antioxidant activity. *LWT - Food Science and Technology, 28*(1), 25–30. https://doi.org/10.1016/S0023-6438(95)80008-5

Chen, X. (2011). Study on structure and thermal stability properties of cellulose fibers from rice straw. *Carbohydrate Polymers*, 6.

Cheung, Y.-C., & Wu, J.-Y. (2013). Kinetic models and process parameters for ultrasound-assisted extraction of water-soluble components and polysaccharides from a medicinal fungus. *Biochemical Engineering Journal, 79*, 214–220. https://doi.org/10.1016/j.bej.2013.08.009

Collazo-Bigliardi, S., Ortega-Toro, R., & Chiralt, A. (2019). Improving properties of thermoplastic starch films by incorporating active extracts and cellulose fibres isolated from rice or coffee husk. *Food Packaging and Shelf Life, 22*, Article 100383. https://doi.org/10.1016/j.fpsl.2019.100383

Derrien, M., Badr, A., Gosselin, A., Desjardins, Y., & Angers, P. (2017). Optimization of a green process for the extraction of lutein and chlorophyll from spinach by-products using response surface methodology (RSM). *LWT - Food Science and Technology, 79*, 170–177. https://doi.org/10.1016/j.lwt.2017.01.010

El-Tayeb, T. S., Abdelhafez, A. A., Ali, S. H., & Ramadan, E. M. (2012). Effect of acid hydrolysis and fungal biotreatment on agro-industrial wastes for obtainment of free sugars for bioethanol production. *Brazilian Journal of Microbiology, 43*(4), 1523–1535. https://doi.org/10.1590/S1517-83822012000400037

Elzaawely, A. A., Maswada, H. F., El-Sayed, M. E. A., & Ahmed, M. E. (2017). Phenolic compounds and antioxidant activity of rice straw extract. *International Letters of Natural Sciences, 64*, 1–9. https://doi.org/10.18052/www.scipress.com/ILNS.64.1

European Bioplastics, nova-Institute (2020). Bioplastics market data. [Web page] Recovered 1st April of 2021 from https://www.european-bioplastics.org/market/.

FAOSTAT . (2018). Retrieved November 4, 2020, from http://www.fao.org/faostat/en/#data/QC/visualize.

Freitas, P. A. V., González-Martínez, C., & Chiralt, A. (2020). Application of ultrasound pre-treatment for enhancing extraction of bioactive compounds from rice straw. *Foods, 9*(11), 1657. https://doi.org/10.3390/foods9111657

Freitas, P. A. V., La Fuente Arias, C. I., Torres-Giner, S., González-Martínez, C., & Chiralt, A. (2021). Valorization of rice straw into cellulose microfibers for the reinforcement of thermoplastic corn starch films. *Applied Sciences*, 11. https://doi.org/10.3390/app11188433

Freitas, P. A. V., González-Martínez, C., & Chiralt, A. (2022). Applying ultrasound-assisted processing to obtain cellulose fibres from rice straw to be used as reinforcing agents. *Innovative Food Science & Emerging Technologies*, 76. https://doi.org/10.1016/j.ifset.2022.102932

Han, J.-W., Ruiz-Garcia, L., Qian, J.-P., & Yang, X.-T. (2018). Food packaging: A comprehensive review and future trends: Food packaging: Review and future trends. *Comprehensive Reviews in Food Science and Food Safety, 17*(4), 860–877. https://doi.org/10.1111/1541-4337.12343

Hayat, K., Abbas, S., Hussain, S., Shahzad, S. A., & Tahir, M. U. (2019). Effect of microwave and conventional oven heating on phenolic constituents, fatty acids, minerals and antioxidant potential of fennel seed. *Industrial Crops and Products, 140*, Article 111610. https://doi.org/10.1016/j.indcrop.2019.111610

Hernández-García, E., Vargas, M., & Chiralt, A. (2021). Thermoprocessed starch-polyester bilayer films as affected by the addition of gellan or xanthan gum. *Food Hydrocolloids, 113*, Article 106509. https://doi.org/10.1016/j.foodhyd.2020.106509

Hosseini, S. F., Javidi, Z., & Rezaei, M. (2016). Efficient gas barrier properties of multi-layer films based on poly(lactic acid) and fish gelatin. *International Journal of Biological Macromolecules, 92*, 1205–1214. https://doi.org/10.1016/j.ijbiomac.2016.08.034

Lahmass, I., Ouahhoud, S., Elyoubi, M., Benabbas, R., Sabouni, A., Asehraou, A., & Saalaoui, E. (2018). Evaluation of antioxidant activities of saffron stigma and spath as by-product of Crocus sativus L. *MOJ Biology and Medicine, 3*(4), 154–158. https://doi.org/10.15406/mojbm.2018.03.00091

Jamshidian, M., Tehrany, E. A., Imran, M., Akhtar, M. J., Cleymand, F., & Desobry, S. (2012a). Structural, mechanical and barrier properties of active PLA–antioxidant films. *Journal of Food Engineering, 110*(3), 380–389. https://doi.org/10.1016/j.jfoodeng.2011.12.034

Jamshidian, M., Tehrany, E. A., & Desobry, S. (2012b). Release of synthetic phenolic antioxidants from extruded poly lactic acid (PLA) film, 475 *Food Control, 28*(2), 445–455. https://doi.org/10.1016/j.foodcont.2012.05.005.

Jara-Palacios, M. J., Gonçalves, S., Heredia, F. J., Hernanz, D., & Romano, A. (2020). Extraction of antioxidants from winemaking byproducts: Effect of the solvent on phenolic composition, antioxidant and anti-cholinesterase activities, and electrochemical behaviour. *Antioxidants, 9*(8), 675. https://doi.org/10.3390/antiox9080675

Karimi, E., Mehrabanjoubani, P., Keshavarzian, M., Oskoueian, E., Jaafar, H. Z., & Abdolzadeh, A. (2014). Identification and quantification of phenolic and flavonoid components in straw and seed husk of some rice varieties (*Oryza sativa* L.) and their antioxidant properties: Identification and quantification of phenolic and flavonoid. *Journal of the Science of Food and Agriculture, 94*(11), 2324–2330. https://doi.org/10.1002/jsfa.6567

Li, Y., Qi, B., Luo, J., Khan, R., & Wan, Y. (2015). Separation and concentration of hydroxycinnamic acids in alkaline hydrolyzate from rice straw by nanofiltration. *Separation and Purification Technology, 149*, 315–321. https://doi.org/10.1016/j.seppur.2015.06.006

Llana-Ruiz-Cabello, M., Pichardo, S., Baños, A., Núñez, C., Bermúdez, J. M., Guillamón, E., Aucejo, S., & Cameán, A. M. (2015). Characterisation and evaluation of PLA films containing an extract of Allium spp. to be used in the packaging of ready-to-eat salads under controlled atmospheres. *LWT - Food Science and Technology, 64*, 1354–1361. https://doi.org/10.1016/j.lwt.2015.07.057

Lourenço, S. C., Moldão-Martins, M., & Alves, V. D. (2019). Antioxidants of natural plant origins: From sources to food industry applications. *Molecules, 24*(22), 4132. https://doi.org/10.3390/molecules24224132

Marzlan, A. A., Muhialdin, B. J., Zainal Abedin, N. H., Manshoor, N., Ranjith, F. H., Anzian, A., & Meor Hussin, A. S. (2022). Incorporating torch ginger (Etlingera elatior Jack) inflorescence essential oil onto starch-based edible film towards sustainable active packaging for chicken meat. *Industrial Crops and Products, 184*, Article 115058. https://doi.org/10.1016/j.indcrop.2022.115058

Mchugh, T. H., Avena-Bustillos, R., & Krochta, J. M. (1993). Hydrophilic edible films: Modified procedure for water vapor permeability and explanation of thickness effects. *Journal of Food Science, 58*(4), 899–903. https://doi.org/10.1111/j.1365-2621.1993.tb09387.x

Menzel, C., González-Martínez, C., Chiralt, A., & Vilaplana, F. (2019). Antioxidant starch films containing sunflower hull extracts. *Carbohydrate Polymers, 214*, 142–151. https://doi.org/10.1016/j.carbpol.2019.03.022

Menzel, C., González-Martínez, C., Vilaplana, F., Diretto, G., & Chiralt, A. (2020). Incorporation of natural antioxidants from rice straw into renewable starch films. *International Journal of Biological Macromolecules, 146*, 976–986. https://doi.org/10.1016/j.ijbiomac.2019.09.222

Moreno, O., Atarés, L., Chiralt, A., Cruz-Romero, M. C., & Kerry, J. (2018). Starch-gelatin antimicrobial packaging materials to extend the shelf life of chicken breast fillets. *LWT - Food Science and Technology, 97*, 483–490.

Muller, J., Quesada, A. B., González-Martínez, C., & Chiralt, A. (2017a). Antimicrobial properties and released of cinnamaldehyde in bilayer films based on polylatctic acid (PLA) and starch. *European Polymer Journal, 96*, 316–325.

Muller, J., González-Martínez, C., & Chiralt, A. (2017b). Poly(lactic) acid (PLA) and starch bilayer films, containing cinnamaldehyde, obtained by compression moulding. *European Polymer Journal, 95*, 56–70. https://doi.org/10.1016/j.eurpolymj.2017.07.019

Peanparkdee, M., & Iwamoto, S. (2019). Bioactive compounds from by-products of rice cultivation and rice processing: Extraction and application in the food and pharmaceutical industries. *Trends in Food Science & Technology, 86*, 109–117. https://doi.org/10.1016/j.tifs.2019.02.041

Peppas, N. A., & Brannon-Peppas, L. B. (1994). Water Diffusion and sorption in amorphous macromolecular systems and foods. *Journal of Food Engineering, 22*, 189–210. https://doi.org/10.1016/B978-1-85861-037-5.50015-1

Peleg, M. (1988). An empirical model for the description of moisture sorption curves. *Journal of Food 510 Science, 53*(4), 1216–1217. https://doi.org/10.1111/j.1365-2621.1988.tb13565.x

Randhawa, S., & Bahna, S. L. (2009). Hypersensitivity reactions to food additives. *Current Opinion in Allergy & Clinical Immunology, 9*(3), 278–283. https://doi.org/10.1097/ACI.0b013e32832b2632

Requena, R., Vargas, M., & Chiralt, A. (2017). Release kinetics of carvacrol and eugenol from poly(hydroxybutyrate-co-hydroxyvalerate) (PHBV) films for food packaging applications. *European Polymer Journal, 92*, 185–193. https://doi.org/10.1016/j.eurpolymj.2017.05.008

Roy, S., & Rhim, J.-W. (2020). Preparation of bioactive functional poly(lactic acid)/curcumin composite film for food packaging application. *International Journal of Biological Macromolecules, 162*, 1780–1789. https://doi.org/10.1016/j.ijbiomac.2020.08.094

Sato, S., Gondo, D., Wada, T., Kanehashi, S., & Nagai, K. (2013). Effects of various liquid organic solvents on solvent-induced crystallization of amorphous poly(lactic acid) film. *Journal of Applied Polymer Science, 129*(3), 1607–1617. https://doi.org/10.1002/app.38833

Srisa, A., & Harnkarnsujarit, N. (2020). Antifungal films from trans-cinnamaldehyde incorporated poly (lactic acid) and poly(butylene adipate-co-terephthalate) for bread packaging. *Food Chemistry, 333*, Article 127537. https://doi.org/10.1016/j.foodchem.2020.127537

Talón, E., Trifkovic, K. T., Nedovic, V. A., Bugarski, B. M., Vargas, M., Chiralt, A., & González-Martínez, C. (2017). Antioxidant edible films based on chitosan and starch containing polyphenols from thyme extracts. *Carbohydrate Polymers, 157*, 1153–1161. https://doi.org/10.1016/j.carbpol.2016.10.080

Vasile, C., Stoleru, E., Darie-Nita, R. N., Dumitriu, R. P., Pamfil, D., & Tartau, L. (2019). Biocompatible materials based on plasticized poly(lactic acid), chitosan and rosemary ethanolic extract I. Effect of chitosan on the properties of plasticized poly (lactic acid) materials. *Polymers, 11*(6), 1–28. https://doi.org/10.3390/polym11060941

Velásquez, E., Vidal, C. P., Rojas, A., Guarda, A., Galotto, M. J., & Dicastillo, C. L. (2021). Natural antimicrobials and antioxidants added to polylactic acid packaging films. Part I: Polymer processing techniques. *Comprehensive Reviews In Food Science and Food Safety, 20*, 3388–3403.

Vilarinho, F., Stanzione, M., Buonocore, G. G., Barbosa-Pereira, L., Sendón, R., Vaz, M. F., & Sanches Silva, A. (2021). Green tea extract and nanocellulose embedded into polylactic acid film: Properties and efficiency on retarding the lipid oxidation of a model fatty food. *Food Packaging and Shelf Life, 27*, Article 100609. https://doi.org/10.1016/j.fpsl.2020.100609

Yang, H.-H., Tsai, C.-H., Chao, M.-R., Su, Y.-L., & Chien, S.-M. (2006). Source identification and size distribution of atmospheric polycyclic aromatic hydrocarbons during rice straw burning period. *Atmospheric Environment, 40*(7), 1266–1274. https://doi.org/10.1016/j.atmosenv.2005.10.032

Ziemlewska, A., Zagórska-Dziok, M., & Nizioł-Łukaszewska, Z. (2021). Assessment of cytotoxicity and antioxidant properties of berry leaves as by-products with potential application in cosmetic and pharmaceutical products. *Scientific Reports, 11*(1), 3240. https://doi.org/10.1038/s41598-021-82207-2